Cell, Vol. 104, 165–172, January 12, 2001, Copyright ©2001 by Cell Press

Mutations in the Gene Encoding Tight Junction Claudin-14 Cause Autosomal Recessive Deafness *DFNB29*

Edward R. Wilcox,*# Quianna L. Burton,‡ Sadaf Naz,† Saima Riazuddin,*† Tenesha N. Smith,* Barbara Ploplis,* Inna Belyantseva,§ Tamar Ben-Yosef,* Nikki A. Liburd,* Robert J. Morell,* Bechara Kachar,§ Doris K. Wu,‡ Andrew J. Griffith,*‖ Sheikh Riazuddin,† and Thomas B. Friedman*

*Laboratory of Molecular Genetics
5 Research Court
NIDCD/NIH
Rockville, Maryland 20850
†Center of Excellence in Molecular Biology
Punjab University
Lahore
Pakistan
‡Section on Sensory Cell Regeneration & Development
NIDCD/NIH
Rockville, Maryland 20850
§Section on Structural Cell Biology
‖Neuro-Otology Branch
NIDCD/NIH
Bethesda, Maryland 20892

Summary

Tight junctions in the cochlear duct are thought to compartmentalize endolymph and provide structural support for the auditory neuroepithelium. The claudin family of genes is known to express protein components of tight junctions in other tissues. The essential function of one of these claudins in the inner ear was established by identifying mutations in *CLDN14* that cause nonsyndromic recessive deafness *DFNB29* in two large consanguineous Pakistani families. In situ hybridization and immunofluorescence studies demonstrated mouse claudin-14 expression in the sensory epithelium of the organ of Corti.

Introduction

Tight junctions are circumferential seals around cells that selectively modulate paracellular permeability between extracellular compartments, and act as a boundary between the apical and basolateral plasma membrane maintaining epithelial cell polarity. These two aspects of tight junctions are also referred to as the barrier and fence functions, respectively (Furuse et al., 1998a). Tight junctions have been observed in ultrastructural analyses of the cochlea and are thought to be necessary for the extracellular compartmentalization of the inner ear (Jahnke, 1975; Gulley and Reese, 1976). However, the molecular composition of tight junctions in the cochlea is largely unknown.

Tight junction fibrils are composed of any one of at least 20 members of the claudin-encoding genes (Furuse et al., 1998a; Morita et al., 1999; Tsukita and Furuse, 2000). Claudins range from approximately 22–24 kDa with four transmembrane domains, they have significant protein sequence similarity to claudins-1 and -2, and carboxyl termini recognized by PDZ domains of the submembranous plaque proteins ZO-1, -2, -3 (Itoh et al., 1999; Tsukita and Furuse, 2000). Claudin-1 and claudin-2 form adhesion planes (sheets of tight junction linked cells) upon injection of their corresponding cDNA into fibroblasts that normally lack tight junctions (Furuse et al., 1998b; Tsukita and Furuse, 1999). Moreover, the tight junctions of MDCK cells are able to incorporate FLAG or HA-tagged claudins 1–8 into preexisting tight junction strands in vitro (Furuse et al., 1998a; Morita et al., 1999). This evidence provides strong support for the role of at least some of the claudins in tight junctions.

Occludin, the first transmembrane protein to be identified as part of tight junction strands (Furuse et al., 1993), and junction-associated membrane protein (JAM; Martin-Padura et al., 1998) are two additional transmembrane proteins associated with tight junctions (Balda and Matter, 2000). There are many additional peripheral proteins associated with tight junctions including ZO-1, ZO-2, ZO-3, cingulin, symplekin, and 7H6 antigen, (reviewed in Mitic et al., 2000; Gonzalez-Mariscal et al., 2000). The permeability properties of tight junction complexes vary between different epithelia, largely as a function of which claudin and other interacting proteins are present (Claude and Goodenough, 1973; Tsukita and Furuse, 2000).

Claudin-3 and -4 are selectively removed from tight junction strands by *Clostridium perfringens* enterotoxin (*CPE*) causing a change in paracellular flux and thereby demonstrating the direct involvement of claudin-3 and -4 in the barrier function of tight junctions (Sonoda et al., 1999). In kidney tubules, claudins can also play a role in extracellular or paracellular permeability. Mutations in claudin-16 (Paracellin-1) implicate tight junctions in paracellular resorption of Mg^{2+} and Ca^{2+}, but not monovalent cations (Simon et al., 1999; Wong and Goodenough, 1999; Yu, 2000).

The cochlea of the inner ear has two compartments with different ionic compositions (Figure 1). The perilymph of the scala vestibuli and scala tympani is low in K^+ concentration but high in Na^+, similar to cerebrospinal fluid (Ryan et al., 1979). The ionic composition of the endolymph of the scala media is similar to that in an intracellular microenvironment, which is high in K^+ and low in Na^+ (reviewed in Ferrary and Sterkers, 1998). This large K^+ gradient contributes to an 80–100 mV endocochlear potential, attributed in part to Na^+-K^+ ATPase activity in the stria vascularis (Johnstone and Sellick, 1972; Gratton et al., 1997; Stankovic et al., 1997; Souter and Forge, 1998; Marcus and Chiba, 1999). This electrochemical gradient is critical for the depolarization of sensory hair cells, increasing the sensitivity of the mechanically activated transduction channels located at the top of stereocilia (Hudspeth, 1989; Milhaud et al., 1999).

To maintain the high resting potential in the endo-

To whom correspondence should be addressed (e-mail: wilcoxe@nidcd.nih.gov).

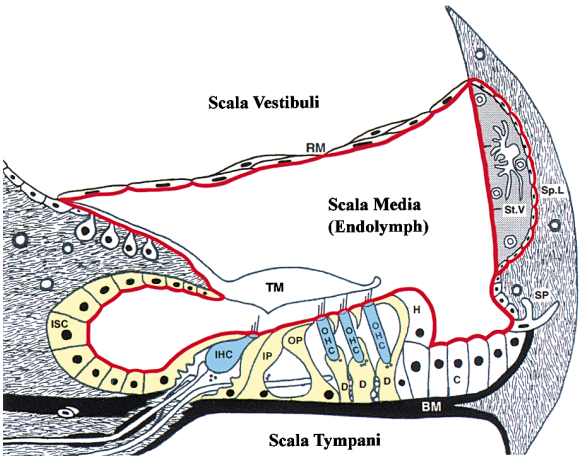

Figure 1. Diagram of the Scalae and Tight Junctional Specializations in the Mammalian Organ of Corti

The solid red line represents the tight junctional barrier surrounding the scala media (endolymph) (Slepecky, 1996). Cells colored blue are positive for *Cldn14* mRNA and protein at postnatal day 4. Cells colored yellow are positive for *Cldn14* at postnatal day 8 (see Figure 5). The reticular lamina, one of the boundaries of the scala media, includes the cuticular plate of the hair cells along with the tops of the interdigiting and flanking phalangeal and Deiters' cells (Gulley and Reese, 1976; Nadol, 1978). The hair cell stereocilia are found protruding into the endolymph of the scala media while the cell bodies are in a fluid accessible to dyes injected into the perilymph of the scala tympani (Ulfendahl et al., 2000). Abbreviations: IHC, inner hair cell; OHC, outer hair cells; IP, inner pillar cell; OP, outer pillar cell; D, Deiters' cells; H, Hensen cells; C, Claudius cells; BM, basilar membrane; ISC, inner sulcus cells; St.V, stria vascularis; Sp.L, spiral ligament; SP, spiral prominence; RM, Reissner's membrane; TM, tectorial membrane. (Adapted from figure 2.2 and 2.3 in Slepecky, 1996, with permission).

lymph, cells bordering this fluid are "sealed" with various types of intercellular tight junctions. For example, nonsensory cells that line the scala media such as the epithelial cells in Reissner's membrane consist of "intermediate to tight" tight junctions versus "very tight" tight junctions found in hair cells and parts of the stria vascularis (Claude and Goodenough, 1973; Jahnke, 1975; Gulley and Reese, 1976; Anniko and Wroblewski, 1984; Bagger-Sjoback et al., 1988).

The importance of claudin-14 in the cochlea is demonstrated by our observations of two different *CLDN14* mutations cosegregating with recessive deafness in two large families with multiple consanguineous intermarriages and the demonstration of specific claudin-14 expression in the sensory epithelium of the cochlea.

Results

The profound, congenital, recessive deafness segregating in families PKSN6 and PKSR9a define a novel locus, *DFNB29*, on chromosome 21q22.1 (Figure 2A). Families PKSN6 and PKSR9a support maximum two-point LOD scores of 6.7 at $\theta = 0$ for the marker *D21S1252* and 6.1 at $\theta = 0$ for *D21S2079*, respectively (Figure 2B). The region of homozygosity of marker *D21S2080* in unaffected individual IV:9 and the region of heterozygosity in affected individual IV:6 (family PKSR9a) define a *DFNB29* linkage interval of 228,600 bp. The *DFNB29* critical interval excludes *KCNE1*, encoding a potassium channel, and *CBR1*, encoding a carbonyl reductase, but contains three genes: *CLDN14* (Claudin-14); *KIAA0136*, a gene of unknown function; and *CHAF1B* (chromatin assembly factor 1B-p60 subunit) (Figure 2C) (Hattori et al., 2000).

Mutations of gap junction proteins encoded by *GJB2* (*Cx26*) and *GJB3* (*Cx31*) are significant causes of deafness (Kelsell et al., 1997; Morell et al., 1998; Xia et al., 1998; Liu et al., 2000). We hypothesized that other proteins with functions important for inner ear cell–cell junctions are essential for hearing and tight junctional proteins are excellent candidates because of the compartmentalization of the cochlea. Claudin-14 was a good candidate for *DFNB29* and thus the sequence of the single protein coding exon of *CLDN14* was examined. Affected individuals in family PKSN6 were found to have a homozygous single nucleotide deletion, 398delT (Figure 3A) within codon Met133, which is located in transmembrane domain 3. This frameshift is predicted to cause premature translation termination 69 nucleotides later, after the substitution of 23 incorrect amino acids and the loss of almost half of the predicted protein. Family PKSR9a cosegregates a missense mutation (T254A) substituting aspartic acid for valine (V85D) (Figure 3B). Valine 85 is conserved among 12 of the 20 claudins, while isoleucine is present among five claudins, and the remaining three claudins have either a cysteine or proline at this position of the consensus molecule (Figure 3C). Aspartic acid at position 85 is predicted to affect hydrophobicity and disrupt the predicted secondary structures in transmembrane domain 2 (Chou and Fasman, 1974a, 1974b; Kyte and Doolittle, 1982).

To determine the allele frequencies of 398delT and T254A, we sequenced *CLDN14* from normal-hearing individuals. Neither 398delT nor T254A was detected in 150 normal control DNA samples (300 chromosomes) from individuals living in Lahore, Pakistan. This indicates that these two variants are not common polymorphisms in the Pakistani population. Moreover, among 100 Pakistani families that could support statistically significant linkage of recessive nonsyndromic deafness (Friedman et al., 2000), only these two families segregated deafness that linked to *CLDN14*. Therefore, mutations of *CLDN14* are unlikely to account for a majority of recessive, nonsyndromic deafness in Pakistan, which is genetically heterogeneous (Riazuddin et al., 2000; Bork et al., 2001)

To understand transcription of claudin-14 more fully, *CLDN14* was amplified by RACE from human liver cDNA (Marathon-ready, Clontech Laboratories, Inc. CA). A comparison of the genomic chromosome 21 sequence with cDNA sequence indicated that *CLDN14* has three exons. We identified two splice isoforms, one with and one without exon 2. The first two *CLDN14* exons have translation termination stops in all three reading frames. The translation start codon is in exon 3 and has Kozak consensus context (Kozak, 1996).

The expression of *CLDN14* mRNA in various human tissues was examined. A Northern blot analysis of *CLDN14* demonstrated expression in human liver and

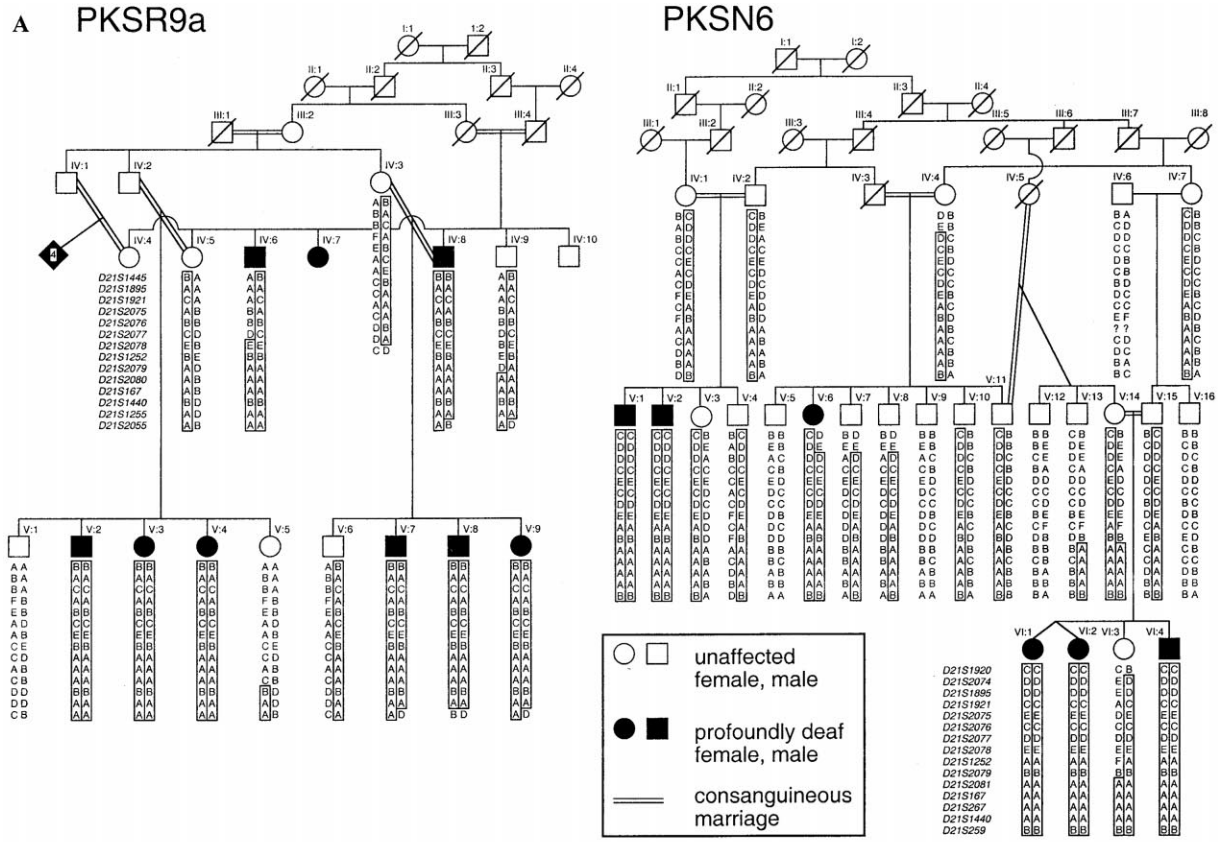

B

Maximum 2 point LOD scores

	PKSR9a		PKSN6	
Marker	LOD	θ	LOD	θ
D21S2077	3.35	0.05	4.45	0
D21S2078	5.70	0	5.40	0
D21S1252	5.16	0	6.74	0
D21S2079	6.08	0	4.65	0

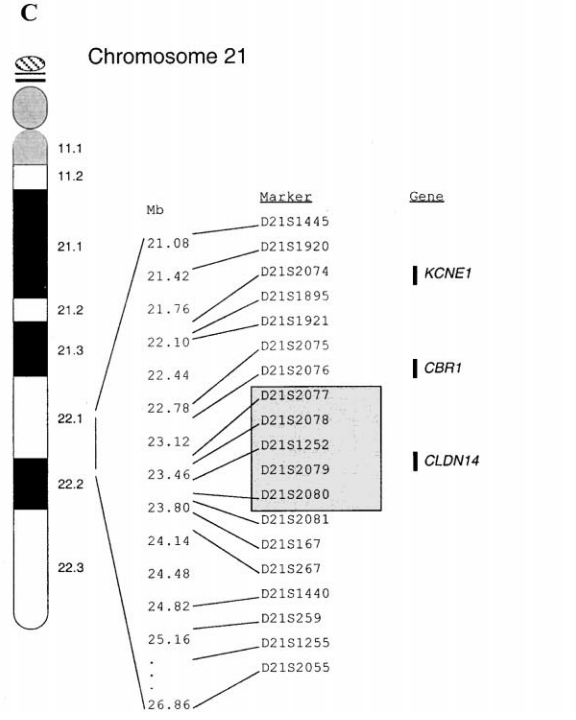

Figure 2. Linkage Information for *DFNB29*

(A) Haplotypes for two large consanguineous families at *DFNB29*. The *DFNB29* critical interval is defined by meiotic recombinations in unaffected persons IV:9 in family PKSR9a, V:14 and VI:3 in family PKSN6, and by the affected person IV:6 in family PKSR9a. The *DFNB29* linkage interval is 228,600 bp in length.

(B) LOD scores for linked genetic markers in the *DFNB29* interval.

(C) The grayed box correlates the *DFNB29* critical linkage region to the DNA sequence from chromosome 21. The DNA sequence for chromosome 21 is marked in megabases (Mb) along one side of a representation of chromosome 21. Markers and genes in the region are tied to the DNA sequence scale showing approximate localizations.

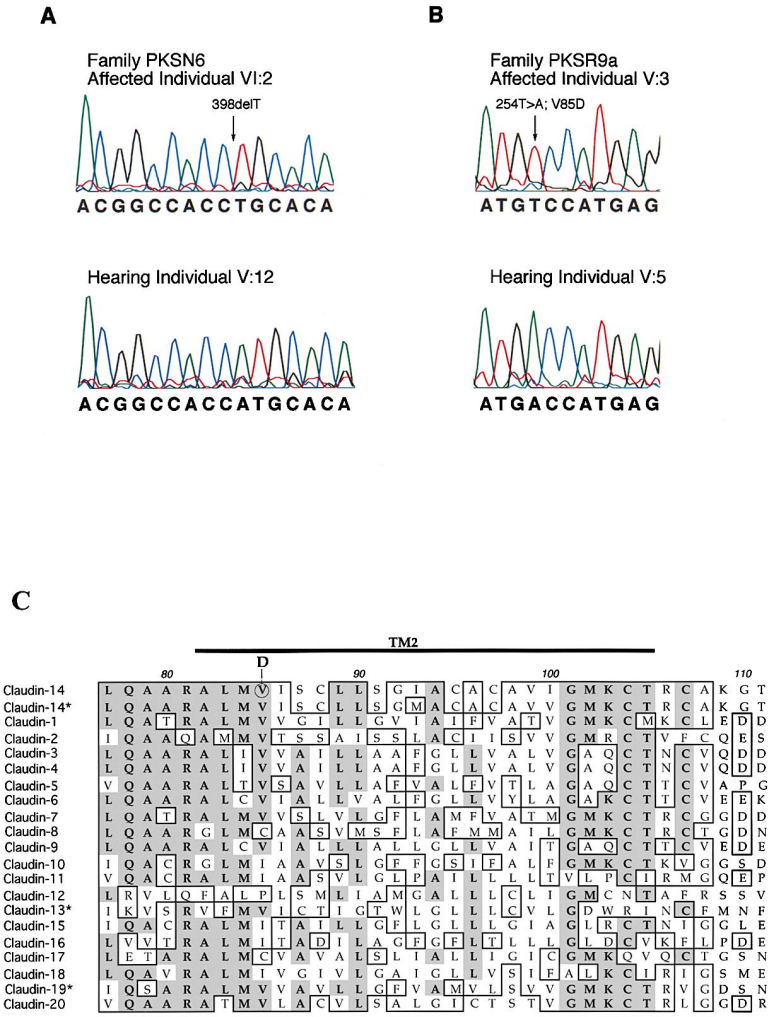

Figure 3. DNA Sequence of Claudin-14

(A) DNA sequence from deaf individual VI:2 of family PKSN6. Notice the missing base "A," as this is the reverse complement of 1258–1273 (398delT) with arrow as compared to the DNA sequence from normal-hearing noncarrier individual V:12 of the PKSN6 family.

(B) DNA sequence from deaf individual V:3 of the PKSR9a family. This is the reverse complement of bases 1112–1123. The affected individual is homozygous for an A > T (254 T > A) transversion (arrow) resulting in the substitution of aspartic acid (D) for valine (V), V85D. The DNA sequence from a normal-hearing noncarrier V:5 in family PKSR9a is shown.

(C) Clustal W comparison of the deduced amino acid sequence of transmembrane domain 2 (TM2) of 21 claudins. The circled valine (V85) of *CLDN14* is an aspartic acid (D) in deaf individuals from family PKSR9a. Aspartic acid is predicted to disrupt the hydrophobicity of the region, as well as the predicted α and β regions in TM2.

kidney (Figure 4). An expression array with poly(A)$^+$ RNA from 75 different human tissues (Clontech Laboratories, Inc. CA) confirmed that liver and kidney express easily detectable quantities of *CLDN14* mRNA. There is no detectable hybridization signal with a *Cldn14* probe on a Northern blot of mouse brain poly(A)$^+$ RNA. *Cldn14* is detected by RT-PCR in mouse brain cDNA with a deduced cDNA sequence of 1456 bp (GenBank accession number AF314089). The physiological significance of low levels of claudin-14 message in the brain and a variety of other cell types is unknown. A *CLDN14* EST is found in a fetal liver-spleen cDNA library (gb|W90592), and an additional clone is found in a pancreatic adenocarcinoma cDNA library (gb|AW471454). RACE results from placenta cDNA amplified a 3′ untranslated sequence matching the gb|AW471454 3′ UTR.

The developmental profile and cell-specific expression of *Cldn14* was further investigated in the mouse inner ear using in situ hybridization and immunocytochemistry. Hybridization with a *Cldn14* RNA probe was not observed at embryonic days 15 or 17, but was detectable at postnatal days 4 and 8 (Figure 5). At postnatal day 4, *Cldn14* hybridization was apically located in the inner and outer hair cell region of the entire organ of Corti (Figures 5A and 5C). As a control, an adjacent section to the one shown in Figure 5A was probed with *Lunatic fringe* (*Lfng*), a marker for the supporting cells of the organ of Corti (Figure 5B; Morsli et al., 1998). *Lfng* is a putative glycosyltransferase involved in the Notch signaling pathway for boundary formation during development (Munro and Freeman, 2000). In the organ of Corti, *Lfng* hybridization signal spanned the entire thickness of the epithelium with a high concentration in the basal region, in contrast to the apical hybridization pattern of *Cldn14*. At postnatal day 8, *Cldn14* mRNA hybridization signal was highest in the supporting cells of the organ of Corti, including the pillar, Deiters', and inner sulcus cells (PC and ISC in Figure 5D). In situ hybridization and immunofluorescence studies both demonstrated *Cldn14* expression in all of the other sensory epithelium of the vestibular organs of the inner ear, including the crista ampullaris and the saccular and utricular maculae. *Cldn14* expression was not detected in nonsensory tissues such as the stria vascularis and Reissner's membrane. Affinity-purified *Cldn14* antibodies demonstrated a cell type-specific pattern of claudin-14 protein expression similar to the results from in situ hybridization described above (Figures 5E–5H). Between postnatal days 4 and 8, claudin-14 diminished in the hair cells and appeared in the supporting cells of the organ of Corti (Figures 1, 5E, and 5F).

Cldn14 is expressed in both the auditory (organ of

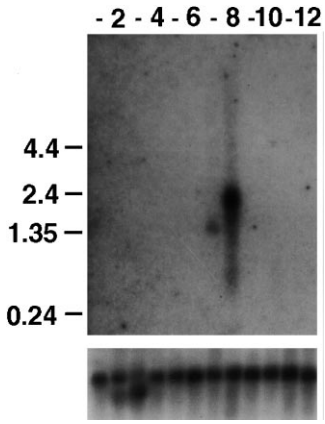

Figure 4. Northern Blot Analysis of Human Claudin-14

Each lane contains approximately 1 μg of human poly(A)$^+$ RNA (Clontech Laboratories, Inc., CA). The following tissues are represented: 1, brain (whole); 2, heart; 3, skeletal muscle; 4, colon (no mucosa); 5, thymus; 6, spleen; 7, kidney; 8, liver; 9, small intestine; 10, placenta; 11, lung; 12, peripheral blood leukocyte. The 335 bp probe is from the 3′ untranslated region of *CLDN14*, nucleotides 1601–1935, GenBank accession number AF314090. The lower panel is the same blot, probed with G3PDG (glyceraldehyde-3-phosphate dehydrogenase, Clontech Laboratories, Inc., CA) demonstrating approximately equivalent amounts of intact RNA in all lanes. The kidney transcript is shorter than that found in liver, indicating that there are additional splice variants of *CLDN14*.

Corti, Figure 5) and vestibular sensory neuroepithelia of the inner ear (data not shown). The sensory organs of balance also have hair cells, K^+-rich endolymph, and a positive electrical potential. We also observed *CLDN14*/*Cldn14* expression in the liver and kidney. However, none of the deaf individuals in families PKSN6 and PKSR9a (aged 4 to 52 years) have reported vestibular disturbances, delays in development of gross motor skills, or signs or symptoms of hepatic or renal dysfunction, thus implying that the liver, kidney, and vestibular organs are functionally unaffected while the organ of Corti is unable to compensate for the loss of claudin-14 function.

Discussion

We describe mutations in *CLDN14* that will disrupt the predicted protein and are associated with profound congenital deafness. In the cochlea, the expression of *Cldn14* is restricted to the organ of Corti and not in other regions of the membranous labyrinth, in agreement with ultrastructural evidence that multiple types of tight junctional complexes are present in the cochlea. We find expression of *Cldn14* mRNA as early as postnatal day 4, with increasing amounts of message by postnatal day 8. This pattern of *Cldn14* expression coincides with the development of the endocochlear potential during the first postnatal week, suggesting that *Cldn14* expression may be required for this latter process (Anniko and Bagger-Sjoback, 1982; Ryan and Woolf, 1983; Souter and Forge, 1998). We hypothesize that claudin-14 is present in a subset of tight junctions of the organ of Corti that are essential for maintaining the electrochemical gradient between the endolymph and its surrounding tissues. This hypothesis will be tested in a *Cldn14* null mouse, which will also be used to examine, by electron microscopy, cochlear tight junctions.

CLDN14 is one of many genes located in the Down syndrome critical region (Shapiro, 1997, 1999). Adult Down syndrome patients have been reported to develop presbycusis at an earlier age than other mentally impaired individuals or cognitively normal individuals (Buchanan, 1990; Hassmann et al., 1998). The contribution of overexpression of *CLDN14* due to a third copy of this gene in trisomy 21 to the etiology of age-related sensorineural hearing loss in Down syndrome patients might be addressed with transgenic mice overexpressing *Cldn14*.

The stria vascularis is necessary for the ionic composition and electrical potential of endolymph. The stria vascularis has two tight junction barriers, one along the marginal cells facing endolymph and the second interconnecting the basal cells, thus creating a separate enclosed intrastrial compartment that does not mix with either perilymph or endolymph (Luciano et al., 1995). The basal cells of the stria vascularis, along with CNS myelin sheaths, are two of a small number of tissues expressing parallel-array tight junction strands (Schnapp and Mugnaini, 1978; Gow et al., 1999). In *Osp/claudin-11* null mice, these parallel tight junctions between basal cells are missing (Gow et al., 1999). Although the auditory phenotype of these mice was not reported, it is of great interest to determine the requirement for claudin-11 in auditory function.

In at least some tissues, a single claudin may be sufficient and essential to form tight junctions (Gow et al., 1999). Conversely, tight junction studies in mouse liver show that different claudin family members (claudin-1 and -3, claudin-1 and -2, and claudin-2 and -3) can be coassembled in a tight junction complex (Furuse et al., 1999). Genetic and biochemical analyses of single claudins are beginning to elucidate the tissue-specific requirements of each claudin family member for tight junction assembly and function.

Experimental Procedures

Genotyping and Linkage Analysis Methods

IRB approval (OH93-DC-016) was obtained for this study from both the National Institutes of Health (NIH) and from the Center of Excellence in Molecular Biology, Lahore, Pakistan. Informed consent was obtained for families from Pakistan. Genomic DNA was subsequently extracted from blood according to a standard protocol (Grimberg et al., 1989).

Many affected individuals in family PKSN6 were homozygous for chromosome 21 markers at the *DFNB10* locus, which was recently identified as a serine protease TMPRSS3 (Scott et al., 2001; T. Ben-Yosef et al., submitted). On refining linkage of deafness in family PKSN6, the *DFNB10* interval was excluded and a new more centromeric locus, *DFNB29*, was mapped. The *DFNB10* locus is at 21q22.3, close to the marker *D21S1890* (52.50 cM on the Marshfield linkage map, http://research.marshfieldclinic.org/genetics/) (Bonne-Tamir et al., 1996; Broman et al., 1998; Berry et al., 2000) while *DFNB29* is 17 cM more proximal at *D21S1252*, (35.45 cM on the Marshfield linkage map), a marker closely linked to *CLDN14*. LOD scores were calculated using FASTLINK (v4.1p) (Schaffer et al., 1994). Deafness was modeled as an autosomal recessive trait. Marker allele frequencies were determined by genotype analysis of genomic DNA from 90 unrelated Pakistani subjects.

PCR Amplification of Family DNA Samples and Mutational Analysis

The single coding exon of *CLDN14* (exon 3) was PCR amplified in two overlapping fragments. The first primer is 5′-AGGAGCGGCGT

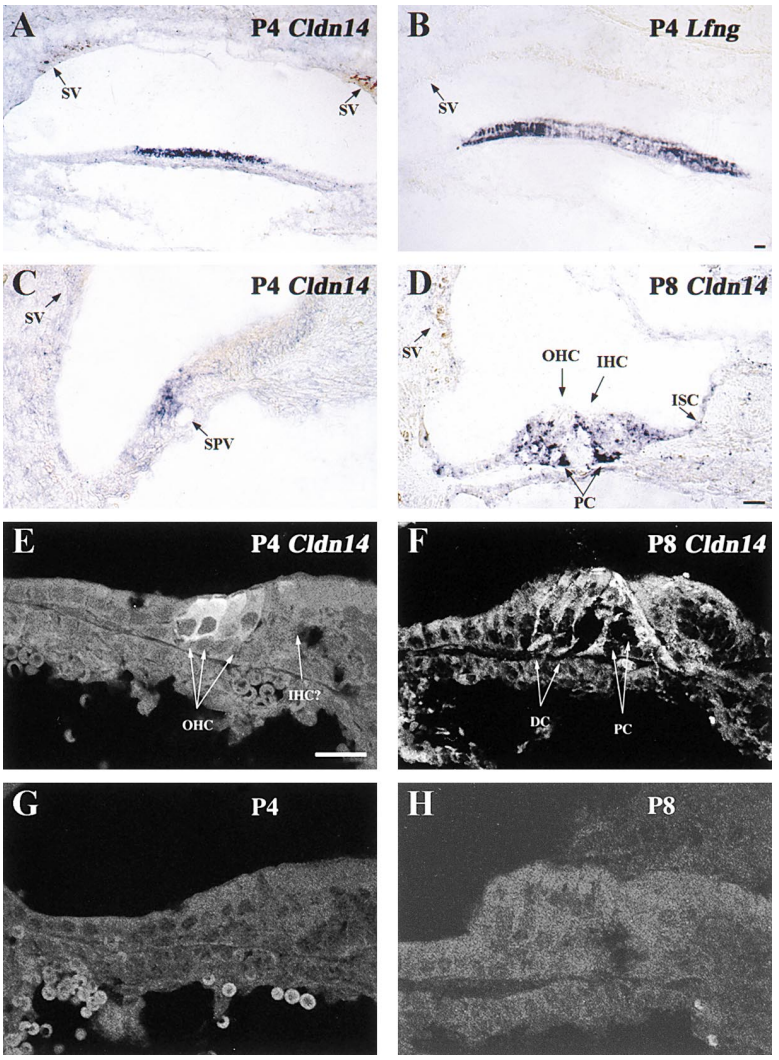

Figure 5. In Situ Hybridization and Immunocytochemistry of Mouse Claudin-14 in the Inner Ear

Frozen 12 μm sections of mouse cochlea at postnatal day 4 (A, B, C, E, and G) and postnatal day 8 (D, F, and H) were processed for in situ hybridization (A–D) and immunostaining (E–H). Adjacent tangential sections of the mouse cochlea at postnatal day 4 were probed for *Cldn14* (A) or lunatic fringe (*Lfng*) (B) mRNA expression. *Lfng* is a marker for the supporting cells of the organ of Corti. *Cldn14* expression is apically located in the hair cell region of the entire organ of Corti (cross section in [C]), whereas *Lfng* expression spans the entire epithelium in the supporting cell region. The supporting cells (inner and outer pillar cells, Deiters' cells) have processes that extend to the reticular lamina (B). At postnatal day 8, *Cldn14* hybridization signals are found broadly within the organ of Corti, with the highest concentration in the pillar cells (PC). Immunofluorescence labeling of the sections from the same cochlea, which were processed for in situ hybridization, revealed a similar pattern of *Cldn14* expression in the sensory epithelium of the organ of Corti (E and F). At postnatal day 4, the labeling is concentrated predominantly in outer hair cells (E). At postnatal day 8, the fluorescence labeling is more prominent in the inner and outer pillar cells and Deiters' cells (F). No labeling in the sensory epithelium of the organ of Corti was observed when the samples were preincubated with an excess of immunogenic peptide (G and H). Scale bar (50 μm) in (B) applies to (A). Scale bar (50 μm) in (D) applies to (C). Scale bar (20 μm) in (E) applies to (F), (G), and (H). Abbreviations: DC, Deiters' cells; IHC, inner hair cells; ISC, inner sulcus cells; OHC, outer hair cells; PC, pillar cells; SPV, spiral vessel; SV, stria vascularis. See Figure 1 for a schematic diagram of the organ of Corti.

GACCC-3′ paired with 5′-TGCCACCAATGAGCGAGAG-3′; the second primer is 5′-CGCGCCCTCATGGTCATCT-3′ paired with 5′-CCC CCTCTGTCCCTGTGCT-3′, GenBank accession number AF314090. Before DNA sequencing but after PCR amplification, the reaction was digested with exonuclease I/shrimp alkaline phosphatase to remove unincorporated nucleotides and primers. DNA sequencing was performed on an ABI377 with ABI prism BigDye terminator cycle sequencing chemistry (Applied Biosystems, Foster City, CA) and the data were analyzed and compared using DNAstar (DNASTAR, Inc. Madison, WI), MacVector v.7 (Oxford Molecular Group, Inc., Campbell, CA), Genotator (Harris, 1997), and phred/phrap/consed (Ewing and Green, 1998; Ewing et al., 1998; Gordon et al., 1998).

Claudin-14 Gene Cloning

The full-length *CLDN14* 5′ and 3′ untranslated sequences were PCR amplified from human liver and placenta Marathon-ready cDNA, respectively (Clontech Laboratories, Inc. CA). Claudin-14 coding sequence specific primers were designed from the human and the mouse gene sequences (Accession numbers NM_012130, NM_019500, respectively). The AP1 primer for the human 3′ RACE was 5′-GCGGGTA CAGGCTGAACGACTA-3′ (nt 1558, numbers refer to the 5′ most nucleotide of the oligonucleotide with reference to GenBank accession number AF314090, the sequence deposited from the RACE results). The second primer (AP2) for this nested 3′ RACE reaction was 5′-CTTCTCCCCTGGGCTGCTGT-3′ (nt 1601). The AP1 primer for the human 5′ RACE was 5′-AGGTGGTCTTGGCGGGTGTG-3′ (complement starting at nt 1996). The second human primer (AP2) for this nested 5′ RACE reaction was 5′-GCGGCAGGATGGTGGT GAT-3′ (complement of nt 933). The AP1 primer for the mouse brain 3′ RACE was 5′-CACCAGCGGCCTACAAGGAC-3′ (nt 1170). The second primer (AP2) for this nested 3′ RACE was 5′-GCACAGTGGG TACAGGCTGAATG-3′ (nt 1219). The AP1 primer for the mouse brain 5′ RACE was 5′-GGGGCACGGTTGTCCTTGTAG-3′ (complement starting at nt 1180). The AP2 primer for the mouse brain 5′ RACE was 5′-GAGCTGGACCGCTGTGCTG-3′ (complement starting at nt 538). The PCR amplimers were synthesized with Advantage Polymerase (Clontech Laboratories, Inc., CA) from mouse brain Marathon-ready cDNA (Clontech Laboratories, Inc., Palo Alto, CA), excised from an agarose gel, and cloned into the pGEM®-T Easy Vector (Promega Corp., WI).

In Situ Hybridization

A 1.4 kb cDNA fragment of mouse *Cldn14*, which includes the entire protein coding region, was subcloned into the pGEM®-T Easy Vector and used for generation of sense and antisense RNA probes for in situ hybridizations of 12 μm frozen sections of the inner ear as previously described (Morsli et al., 1998). *Lfng* RNA probes were prepared as described (Morsli et al., 1998). No in situ hybridization signal was detected with the control sense RNA probes.

Antiserum Production/Purification

Cldn14 peptide sequence AAYKDNRAPSVTSATHSGYR (amino acids 215–234) from the carboxy-terminal region was conjugated to key-

hole limpet hemocyanin (Princeton Biomolecules, PA) and was used to raise rabbit antisera (Covance Research Products, Inc., PA). Among the 20 known mouse and human claudins, this peptide is unique to *Cldn14*. Claudin carboxyl termini in general are divergent (Morita et al., 1999). The rabbit antiserum was affinity purified over the peptide mentioned above attached to AminoLink® Plus immobilization coupling gel (Pierce Chemical Corp., Rockford, IL). This antiserum is immunoreactive against the peptide on a Western blot.

Immunofluorescence Methods

Twelve micron frozen sections of the inner ear were rehydrated in PBS and incubated for 1 hr in a blocking PBS solution containing 2% donkey serum (Sigma, Saint Louis, MO) and 2% bovine serum albumin (ICN Biomedicals, Inc., Aurora, OH). Samples were incubated for 2 hr in the affinity-purified *Cldn14* antiserum (0.23 mg/ml), diluted 1:200 v/v in the blocking solution. After several rinses in PBS, the tissue sections were incubated for 40 min with fluorescein-conjugated donkey anti-rabbit IgG secondary antibody (Amersham, Arlington Heights, IL), diluted 1:200 v/v in blocking solution. Samples were rinsed and mounted using ProLong Antifade Kit (Molecular Probes, Eugene, OR). The specificity of labeling was verified by preincubation of the primary antibody (0.23 mg/ml), diluted 1:200 v/v, with an excess of the immunogenic peptide (1 mg/ml), diluted 1:200 v/v, for 2 hr at room temperature. Samples were viewed with a 510 Zeiss Laser Scanning Confocal microscope with 40× objective (N.A. = 1.3).

Clinical Assessment of *CLDN14* Families

After obtaining written informed consent, patient interviews and physical examinations were conducted by a physician (A. J. G.). Special attention was directed toward identification of any symptoms or signs of renal or hepatic dysfunction, but none were observed. Vestibular function was assessed by the tandem gait and Romberg test. Pure-tone air conduction audiometry was performed by Siemens Hearing and Speech Centre, Lahore, Pakistan under ambient noise conditions.

Acknowledgments

We are grateful for the participation of many families living in Pakistan. We also thank Barbara Ploplis for managing LMG databases and markers that made this work possible. We thank Susan Sullivan and Dennis Drayna for their comments on this manuscript and are indebted to Basharat Ullah Amjad, Director of Special Education, Punjab and to the Hamza Foundation Academy for the Deaf. Our study is supported by the National Institute on Deafness and Other Communication Disorders, Intramural Research Project Z01DC00026. University grants commission supported part of this study in Pakistan.

Received October 31, 2000; revised November 28, 2000.

References

Anniko, M., and Bagger-Sjoback, D. (1982). Maturation of junctional complexes during embryonic and early postnatal development of inner ear secretory epithelia. Am. J. Otolaryngol. *3*, 242–253.

Anniko, M., and Wroblewski, R. (1984). The freeze fracture technique in inner ear research. Scan. Electron Microsc. *4*, 2067–2075.

Bagger-Sjoback, D., Engstrom, B., and Hillerdal, M. (1988). Membrane specializations in the human organ of Corti. Acta Otolaryngol. *106*, 19–28.

Balda, M.S., and Matter, K. (2000). Transmembrane proteins of tight junctions. Semin. Cell Dev. Biol. *11*, 281–289.

Berry, A., Scott, H.S., Kudoh, J., Talior, I., Korostishevsky, M., Wattenhofer, M., Guipponi, M., Barras, C., Rossier, C., Shibuya, K., et al. (2000). Refined localization of autosomal recessive nonsyndromic deafness DFNB10 locus using 34 novel microsatellite markers, genomic structure, and exclusion of six known genes in the region. Genomics *68*, 22–29.

Bonne-Tamir, B., DeStefano, A.L., Briggs, C.E., Adair, R., Franklyn, B., Weiss, S., Korostishevsky, M., Frydman, M., Baldwin, C.T., and Farrer, L.A. (1996). Linkage of congenital recessive deafness (gene DFNB10) to chromosome 21q22.3. Am. J. Hum. Genet. *58*, 1254–1259.

Bork, J.M., Peters, L.M., Riazuddin, S., Bernstein, S.L., Ahmed, Z.M., Ness, S.L., Polomeno, R., Ramesh, A., Schloss, M., Srikumari Srisailpathy, C.R., et al. (2001). Usher syndrome 1D and nonsyndromic autosomal recessive deafness DFNB12 are caused by allelic mutations of the novel cadherin-like gene CDH23. Am. J. Hum. Genet. *68*, 26–37.

Broman, K.W., Murray, J.C., Sheffield, V.C., White, R.L., and Weber, J.L. (1998). Comprehensive human genetic maps: individual and sex-specific variation in recombination. Am. J. Hum. Genet. *63*, 861–869.

Buchanan, L.H. (1990). Early onset of presbyacusis in Down syndrome. Scand. Audiol. *19*, 103–110.

Chou, P.Y., and Fasman, G.D. (1974a). Conformational parameters for amino acids in helical, beta-sheet, and random coil regions calculated from proteins. Biochemistry *13*, 211–222.

Chou, P.Y., and Fasman, G.D. (1974b). Prediction of protein conformation. Biochemistry *13*, 222–245.

Claude, P., and Goodenough, D.A. (1973). Fracture faces of zonulae occludentes from "tight" and "leaky" epithelia. J. Cell Biol. *58*, 390–400.

Ewing, B., and Green, P. (1998). Base-calling of automated sequencer traces using phred. II. Error probabilities. Genome Res. *8*, 186–194.

Ewing, B., Hillier, L., Wendl, M.C., and Green, P. (1998). Base-calling of automated sequencer traces using phred. I. Accuracy assessment. Genome Res. *8*, 175–185.

Ferrary, E., and Sterkers, O. (1998). Mechanisms of endolymph secretion. Kidney Int. Suppl. *65*, S98–S103.

Friedman, T., Battey, J., Kachar, B., Riazuddin, S., Noben-Trauth, K., Griffith, A., and Wilcox, E. (2000). Modifier genes of hereditary hearing loss. Curr. Opin. Neurobiol. *10*, 487–493.

Furuse, M., Hirase, T., Itoh, M., Nagafuchi, A., Yonemura, S., and Tsukita, S. (1993). Occludin: a novel integral membrane protein localizing at tight junctions. J. Cell Biol. *123*, 1777–1788.

Furuse, M., Fujita, K., Hiiragi, T., Fujimoto, K., and Tsukita, S. (1998a). Claudin-1 and -2: novel integral membrane proteins localizing at tight junctions with no sequence similarity to occludin. J. Cell Biol. *141*, 1539–1550.

Furuse, M., Sasaki, H., Fujimoto, K., and Tsukita, S. (1998b). A single gene product, claudin-1 or -2, reconstitutes tight junction strands and recruits occludin in fibroblasts. J. Cell Biol. *143*, 391–401.

Furuse, M., Sasaki, H., and Tsukita, S. (1999). Manner of interaction of heterogeneous claudin species within and between tight junction strands. J. Cell Biol. *147*, 891–903.

Gonzalez-Mariscal, L., Betanzos, A., and Avila-Flores, A. (2000). MAGUK proteins: structure and role in the tight junction. Semin. Cell Dev. Biol. *11*, 315–324.

Gordon, D., Abajian, C., and Green, P. (1998). Consed: a graphical tool for sequence finishing. Genome Res. *8*, 195–202.

Gow, A., Southwood, C.M., Li, J.S., Pariali, M., Riordan, G.P., Brodie, S.E., Danias, J., Bronstein, J.M., Kachar, B., and Lazzarini, R.A. (1999). CNS myelin and sertoli cell tight junction strands are absent in Osp/claudin-11 null mice. Cell *99*, 649–659.

Gratton, M.A., Smyth, B.J., Lam, C.F., Boettcher, F.A., and Schmiedt, R.A. (1997). Decline in the endocochlear potential corresponds to decreased Na,K-ATPase activity in the lateral wall of quiet-aged gerbils. Hear. Res. *108*, 9–16.

Grimberg, J., Nawoschik, S., Belluscio, L., McKee, R., Turck, A., and Eisenberg, A. (1989). A simple and efficient non-organic procedure for the isolation of genomic DNA from blood. Nucleic Acids Res. *17*, 8390.

Gulley, R.L., and Reese, T.S. (1976). Intercellular junctions in the reticular lamina of the organ of Corti. J. Neurocytol. *5*, 479–507.

Harris, N.L. (1997). Genotator: a workbench for sequence annotation. Genome Res. *7*, 754–762.

Hassmann, E., Skotnicka, B., Midro, A.T., and Musiatowicz, M.

(1998). Distortion products otoacoustic emissions in diagnosis of hearing loss in Down syndrome. Int. J. Pediatr. Otorhinolaryngol. *45*, 199–206.

Hattori, M., Fujiyama, A., Taylor, T.D., Watanabe, H., Yada, T., Park, H.S., Toyoda, A., Ishii, K., Totoki, Y., Choi, D.K., et al. (2000). The DNA sequence of human chromosome 21. The chromosome 21 mapping and sequencing consortium. Nature *405*, 311–319.

Hudspeth, A.J. (1989). How the ear's works work. Nature *341*, 397–404.

Itoh, M., Furuse, M., Morita, K., Kubota, K., Saitou, M., and Tsukita, S. (1999). Direct binding of three tight junction-associated MAGUKs, ZO-1, ZO-2, and ZO-3, with the COOH termini of claudins. J. Cell Biol. *147*, 1351–1363.

Jahnke, K. (1975). The fine structure of freeze-fractured intercellular junctions in the guinea pig inner ear. Acta Otolaryngol. Suppl. *336*, 1–40.

Johnstone, B.M., and Sellick, P.M. (1972). The peripheral auditory apparatus. Q. Rev. Biophys. *5*, 1–57.

Kelsell, D.P., Dunlop, J., Stevens, H.P., Lench, N.J., Liang, J.N., Parry, G., Mueller, R.F., and Leigh, I.M. (1997). Connexin 26 mutations in hereditary non-syndromic sensorineural deafness. Nature *387*, 80–83.

Kozak, M. (1996). Interpreting cDNA sequences: some insights from studies on translation. Mamm. Genome *7*, 563–574.

Kyte, J., and Doolittle, R.F. (1982). A simple method for displaying the hydropathic character of a protein. J. Mol. Biol. *157*, 105–132.

Liu, X.Z., Xia, X.J., Xu, L.R., Pandya, A., Liang, C.Y., Blanton, S.H., Brown, S.D., Steel, K.P., and Nance, W.E. (2000). Mutations in connexin31 underlie recessive as well as dominant non-syndromic hearing loss. Hum. Mol. Genet. *9*, 63–67.

Luciano, L., Reiss, G., Iurato, S., and Reale, E. (1995). The junctions of the spindle-shaped cells of the stria vascularis: a link that completes the barrier between perilymph and endolymph. Hear. Res. *85*, 199–209.

Marcus, D.C., and Chiba, T. (1999). K^+ and Na^+ absorption by outer sulcus epithelial cells. Hear. Res. *134*, 48–56.

Martin-Padura, I., Lostaglio, S., Schneemann, M., Williams, L., Romano, M., Fruscella, P., Panzeri, C., Stoppacciaro, A., Ruco, L., Villa, A., et al. (1998). Junctional adhesion molecule, a novel member of the immunoglobulin superfamily that distributes at intercellular junctions and modulates monocyte transmigration. J. Cell Biol. *142*, 117–127.

Milhaud, P.G., Nicolas, M.T., Bartolami, S., Cabanis, M.T., and Sans, A. (1999). Vestibular semicircular canal epithelium of the rat in culture on filter support: polarity and barrier properties. Pflugers Arch. *437*, 823–830.

Mitic, L.L., Van Itallie, C.M., and Anderson, J.M. (2000). Molecular physiology and pathophysiology of tight junctions I. Tight junction structure and function: lessons from mutant animals and proteins. Am. J. Physiol. Gastrointest. Liver Physiol. *279*, G250–G254.

Morell, R.J., Kim, H.J., Hood, L.J., Goforth, L., Friderici, K., Fisher, R., Van Camp, G., Berlin, C.I., Oddoux, C., Ostrer, H., et al. (1998). Mutations in the connexin 26 gene (GJB2) among Ashkenazi Jews with nonsyndromic recessive deafness. N. Engl. J. Med. *339*, 1500–1505.

Morita, K., Furuse, M., Fujimoto, K., and Tsukita, S. (1999). Claudin multigene family encoding four-transmembrane domain protein components of tight junction strands. Proc. Natl. Acad. Sci. USA *96*, 511–516.

Morsli, H., Choo, D., Ryan, A., Johnson, R., and Wu, D.K. (1998). Development of the mouse inner ear and origin of its sensory organs. J. Neurosci. *18*, 3327–3335.

Munro, S., and Freeman, M. (2000). The notch signalling regulator fringe acts in the Golgi apparatus and requires the glycosyltransferase signature motif DXD. Curr. Biol. *10*, 813–820.

Nadol, J.B., Jr. (1978). Intercellular junctions in the organ of Corti. Ann. Otol. Rhinol. Laryngol. *87*, 70–80.

Riazuddin, S., Castelein, C.M., Ahmed, Z.M., Lalwani, A.K., Mastroianni, M.A., Naz, S., Smith, T.N., Liburd, N.A., Friedman, T.B., Griffith, A.J., et al. (2000). Dominant modifier *DFNM1* suppresses recessive deafness *DFNB26*. Nat. Genet. *26*, 431–434.

Ryan, A.F., Wickham, M.G., and Bone, R.C. (1979). Element content of intracochlear fluids, outer hair cells, and stria vascularis as determined by energy-dispersive roentgen ray analysis. Otolaryngol. Head Neck Surg. *87*, 659–665.

Ryan, A.F., and Woolf, N.K. (1983). Energy dispersive x-ray analysis of inner ear fluids and tissues during the ontogeny of cochlear function. Scan Electron Microsc. *1*, 201–207.

Schaffer, A.A., Gupta, S.K., Shriram, K., and Cottingham, R.W., Jr. (1994). Avoiding recomputation in linkage analysis. Hum. Hered. *44*, 225–237.

Schnapp, B., and Mugnaini, E. (1978). Membrane architecture of myelinated fibers as seen by freeze-fracture. In Physiology and Pathobiology of Axons, S.G. Waxman, ed. (New York: Raven Press), pp. 83–123.

Scott, H.S., Kudoh, J., Wattenhofer, M., Shibuya, K., Berry, A., Chrast, R., Guipponi, M., Wang, J., Kawasaki, K., Asakawa, S., et al. (2001). Insertion of β-satellite repeats identifies a transmembrane protease causing both congenital and childhood onset autosomal recessive deafness (DFNB1/10). Nat. Genet., in press.

Shapiro, B.L. (1997). Whither Down syndrome critical regions? Hum. Genet. *99*, 421–423.

Shapiro, B.L. (1999). The Down syndrome critical region. J. Neural. Transm. Suppl. *57*, 41–60.

Simon, D.B., Lu, Y., Choate, K.A., Velazquez, H., Al-Sabban, E., Praga, M., Casari, G., Bettinelli, A., Colussi, G., Rodriguez-Soriano, J., et al. (1999). Paracellin-1, a renal tight junction protein required for paracellular Mg^{2+} resorption. Science *285*, 103–106.

Slepecky, N.B. (1996). Structures of the mammalian cochlea. In The Cochlea, P. Dallos, A.N. Popper, and R.R. Fay, eds. (New York: Springer), pp. 44–129.

Sonoda, N., Furuse, M., Sasaki, H., Yonemura, S., Katahira, J., Horiguchi, Y., and Tsukita, S. (1999). Clostridium perfringens enterotoxin fragment removes specific claudins from tight junction strands: Evidence for direct involvement of claudins in tight junction barrier. J. Cell Biol. *147*, 195–204.

Souter, M., and Forge, A. (1998). Intercellular junctional maturation in the stria vascularis: possible association with onset and rise of endocochlear potential. Hear. Res. *119*, 81–95.

Stankovic, K.M., Brown, D., Alper, S.L., and Adams, J.C. (1997). Localization of pH regulating proteins H+ATPase and Cl-/HCO3- exchanger in the guinea pig inner ear. Hear. Res. *114*, 21–34.

Tsukita, S., and Furuse, M. (1999). Occludin and claudins in tight-junction strands: leading or supporting players? Trends Cell Biol. *9*, 268–273.

Tsukita, S., and Furuse, M. (2000). Pores in the wall: claudins constitute tight junction strands containing aqueous pores. J. Cell Biol. *149*, 13–16.

Ulfendahl, M., Scarfone, E., Flock, A., Le Calvez, S., and Conradi, P. (2000). Perilymphatic fluid compartments and intercellular spaces of the inner ear and the organ of Corti. Neuroimage *12*, 307–313.

Wong, V., and Goodenough, D.A. (1999). Paracellular channels! Science *285*, 62.

Xia, J.H., Liu, C.Y., Tang, B.S., Pan, Q., Huang, L., Dai, H.P., Zhang, B.R., Xie, W., Hu, D.X., Zheng, D., et al. (1998). Mutations in the gene encoding gap junction protein beta-3 associated with autosomal dominant hearing impairment. Nat. Genet. *20*, 370–373.

Yu, A.S. (2000). Paracellular solute transport: more than just a leak? Curr. Opin. Nephrol. Hypertens. *9*, 513–515.

GenBank Accession Numbers

The GenBank accession numbers for the full-length human and mouse gene sequences reported in this paper are AF314090 and AF314089, respectively.